VOLUME 119, NUMBER 31
AUGUST 6, 1997

JOURNAL OF THE AMERICAN CHEMICAL SOCIETY

Aminothiotyrosine Disulfide, an Optical Trigger for Initiation of Protein Folding

Helen S. M. Lu,[†] Martin Volk,[‡,§] Yuriy Kholodenko,[‡] Edward Gooding,[‡] Robin M. Hochstrasser,[‡] and William F. DeGrado*,[†]

Contribution from the Department of Biochemistry and Biophysics, The Johnson Foundation of Research in Biophysics, Department of Chemistry, The University of Pennsylvania, Philadelphia, Pennsylvania 19104

Received February 21, 1997[⊗]

Abstract: The development of an optical trigger for protein folding is described. The optical trigger is an aryl disulfide embedded in a polypeptide such that the aryl disulfide constrains the peptide in a nonhelical conformation. Upon photocleavage of the SS bond, the peptide can then commence to fold into an α-helical conformation. Two thiotyrosine derivatives, (*S*)-4′-mercaptophenylalanine (Tty**)** and 3-*N*-(4′-mercaptophenyl)-(*S*)-2,3-diaminoproprionate (Aty), have been prepared and incorporated into polyalanine peptides. The ease of synthesis of protected forms of Tty and Aty amenable for solid phase synthesis, in four steps with 30% overall yield and six steps in 40% overall yield, respectively, make these attractive candidates as precursors of the optical trigger. CD and IR spectroscopy showed that the cyclic disulfide cross-linked peptides are much less helical than their linear counterparts. Following laser flash photolysis, peptide **7**, which incorporates Tty, showed total recombination of the thiyl radicals within 1 ns. Peptide **16**, which incorporates Aty, showed a significant amount of long-lived thiyl radicals from nanosecond to microsecond time scale. The process of recombination is hypothesized to be governed by the peptide conformation. Because of the significant amount of long-lived thiyl radicals generated from cyclic peptide **16**, Aty should prove to be of general utility in the studies of protein folding on a time scale of sub-picoseconds and greater.

Introduction

The mechanism by which proteins fold rapidly into their native state is currently under active theoretical and experimental investigations. The elucidation of protein folding forces and pathways can shed light on how proteins obtain their unique structures and also aid in the design of novel proteins with tailored functions. To study protein folding or unfolding, a triggering event that perturbs a protein from its equilibrium state is required to initiate either folding or unfolding.[1] Until recently, this has mainly been accomplished by stopped-flow mixing techniques that introduce a change of denaturant concentration in the solvent. These techniques typically have a time resolution of a few milliseconds. However, several proteins have been reported to exhibit significant structure before the millisecond or even microsecond time regime.[2−9] The elucidation of the kinetics and structural features associated with the intermediates

[†] The Johnson Foundation of Research in Biophysics.
[‡] Department of Chemistry.
[§] Present address: Institut für Physikalische und Theoretische Chemie, TU München, Lichtenbergsr. 4, 85748 Garching, Germany.
[⊗] Abstract published in *Advance ACS Abstracts*, July 15, 1997.

(1) Eaton, W. A.; Thompson, P. A.; Chan, C.-K.; Hagen, S. J.; Hofrichter, J. *Structure* **1996**, *4*, 1133−1139.
(2) Bycroft, M.; Matouschek, A.; Kellis, J. T., Jr.; Serrano, L.; Fersht, A. R. *Nature* **1990**, *346*, 488−490.
(3) Houry, W. A.; Rothwarf, D. M.; Scheraga, H. A. *Nature Struct. Biol.* **1995**, *2*, 495−503.
(4) Elöve, G. A.; Chaffotte, A. F.; Roder, H.; Goldberg, M. E. *Biochemistry* **1992**, *31*, 6876−6883.
(5) Jennings, P. A.; Wright, P. E. *Science* **1993**, *262*, 892−895.
(6) Kragelund, B. B.; Robinson, C. V.; Knudsen, J.; Dobson, C. M.; Poulsen, F. M. *Biochemistry* **1995**, *34*, 7217−7224.
(7) Kuwajima, K.; Yamaya, H.; Miwa, S.; Sugai, S.; Nagamura, T. *FEBS Lett.* **1987**, *221*, 115−118.

S0002-7863(97)00567-2 CCC: $14.00

Scheme 1. Photoinitiation of α-Helix Formation

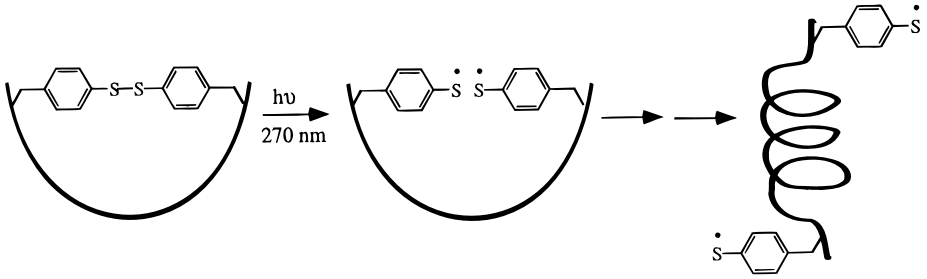

formed in the dead time of the mixing experiments remains a great challenge. In particular, secondary structural elements are often observed to form rapidly in the so-called burst phase of protein folding.

The roles that secondary structure plays in guiding protein folding is under debate. The framework model and the diffusion−collision model[10−15] propose that the secondary structures are formed first, and thereby narrow the conformational search space so that the protein can fold in finite time. Other models of protein folding, such as the hydrophobic collapse model[16] and the nuclear condensation model,[17−20] maintain that collapse of hydrophobic groups or the formation of a group of nuclei occurs first. These interactions then guide the protein to its native state, with secondary structures forming following the rate-determining step. Recent theoretical models of protein folding based on statistical mechanics suggest that secondary structural elements can reduce the number of configurations available to the protein and thus enable rapid folding.[21] In order to resolve these critical issues, an ultrafast trigger to initiate protein folding is required to enable the study of the full range of conformational changes starting from the earliest to the last events of folding.

Different approaches have been utilized to initiate and study the early phases of protein folding. They include temperature jump experiments using short laser pulses to heat the sample to induce either protein unfolding or folding,[22−25] light-initiated ligand dissociation of cytochrome *c*[26] and hemoglobin,[27] and electron transfer induced folding of cytochrome *c*.[28] However, these techniques have their limitations. Temperature jump experiments can only be used to study either the unfolding of proteins, or the folding of proteins that undergo cold denaturation, whereas the light-initiated ligand dissociation and electron transfer initiated folding are limited to hemoproteins. In this work, we set out to develop an ultrafast trigger of protein folding applicable to a wide range of peptides and proteins.

The ideal trigger should be faster than the underlying conformational processes being studied and be readily formed, detected, and incorporated into proteins. Also the photo-triggering event should be reversible to allow for multiple excitations by the laser, enabling data averaging for good signal to noise ratio. To meet these criteria, we chose photocleavage of an aromatic disulfide bond as the triggering event. Aromatic disulfides have been shown to cleave in less than 1 ps.[29−31] The resulting thiyl radical is a strong chromophore ($\epsilon_{540} = 9077$ M^{-1} cm^{-1} for *p*-aminophenylthiyl radical[30,32]) which can therefore serve as an optical probe of the protein dynamics. This scheme requires the synthesis of an appropriate thiol-containing amino acid that is amenable to solid phase synthesis. Placement of two of these thiol residues at specific places in a peptide sequence, followed by oxidation of the resulting dithiol-containing peptide to disulfides, should constrain the polypeptide into a non-native conformation. Laser flash photolysis of the polypeptide leads to photocleavage of the S−S bond, and the polypeptide can then commence folding to the native state. This process is illustrated Scheme 1.

As a demonstration of the utility of our trigger, we chose to study the folding of an alanine rich peptide, which has been shown by Marqusee and Baldwin to fold into stable helices in solution.[33] With our trigger incorporated, we should be able to study the early events of helix formation. Following photo-dissociation of the disulfide, conformational changes of the peptide can be followed by transient IR spectroscopy, a very sensitive method that detects bond level changes of protein

(8) Ptitsyn, O. B.; Pain, R. H.; Semisotnov, G. V.; Zerovnik, E.; Razgulayaev, E. I. *FEBS Lett.* **1990**, *262*, 20−24.
(9) Radford, S. E.; Dobson, C. M.; Evans, P. A. *Nature* **1992**, *358*, 302−307.
(10) Karplus, M.; Weaver, D. C. *Nature* **1976**, *260*, 404−406.
(11) Karplus, M.; Weaver, D. L. *Protein Sci.* **1994**, *3*, 650−668.
(12) Kim, P. S.; Baldwin, R. L. *Annu. Rev. Biochem.* **1982**, *51*, 459−489.
(13) Kim, P. S.; Baldwin, R. L. *Annu. Rev. Biochem.* **1990**, *59*, 631−660.
(14) Ptitsyn, O. B. *Protein Eng.* **1994**, *7*, 593−596.
(15) Wetlaufer, D. B. *Proc. Natl. Acad. Sci. U.S.A.* **1973**, *70*, 697−701.
(16) Dill, K. *Biochemistry* **1985**, *24*, 1501−1509.
(17) Abkevich, V. I.; Gutin, A. M.; Shakhnovich, E. I. *Biochemistry* **1994**, *33*, 10026−10036.
(18) Fersht, A. R. *Proc. Natl. Acad. Sci. U.S.A.* **1995**, *92*, 10869−10873.
(19) Sosnick, T. R.; Mayne, L.; Englander, S. W. *Proteins: Struct., Funct., Genet.* **1996**, *24*, 413−426.
(20) Guo, Z.; Thirumalai, D. *Biopolymers* **1995**, *36*, 83−102.
(21) Bryngelson, J. D.; Onuchic, J. N.; Socci, N. D.; Wolynes, P. G. *Proteins* **1995**, *21*, 167−195.
(22) Nölting, B.; Golbik, R.; Fersht, A. R. *Proc. Natl. Acad. Sci. U.S.A.* **1995**, *92*, 10668−10672.
(23) Phillips, C. M.; Mizutani, Y.; Hochstrasser, R. M. *Proc. Natl. Acad. Sci. U.S.A.* **1995**, *92*, 7292−7296.
(24) (a) Williams, S.; Causgrove, T. P.; Gilmanshin, R.; Fang, K. S.; Callender, R. H.; Woodruff, W. H.; Dyer, R. B. *Biochemistry* **1996**, *35*, 691−697. (b) The folding lifetime for helix formation was originally reported to be 16 ns in ref 24a and was subsequently revised to 180 ns in Gilmanshin, R.; Williams, S.; Callender, R. H.; Woodruff, W. H.; Dyer, R. B. *Proc. Natl. Acad. Sci. U.S.A.* **1997**, *94*, 3709−3713.
(25) Ballew, R. M.; Sabelko, J.; Gruebele, M. *Proc. Natl. Acad. Sci. U.S.A.* **1996**, *93*, 5759−5764.
(26) Jones, C. M.; Henry, E. R.; Hu, Y.; Chan, C.-K.; Luck, S. D.; Bhuyan, A.; Roder, H.; Hofrichter, J.; Eaton, W. A. *Proc. Natl. Acad. Sci. U.S.A.* **1993**, *90*, 11860−11864.
(27) Anfinrud, P. A.; Han, C.; Hochstrasser, R. M. *Proc. Natl. Acad. Sci. U.S.A.* **1989**, *86*, 8387−8391.
(28) Pascher, T.; Chesick, J. P.; Winkler, J. R.; Gray, H. B. *Science* **1996**, *271*, 1558−1560.
(29) Borisevich, N. A.; Lysak, N. A.; Melnichuk, S. V.; Tikhomirov, S. A.; Tolstorozhev, G. B. *Fast Structural Transformations of Organic Molecules*; Springer-Verlag: Berlin, 1990; Vol. 49, pp 276−281.
(30) Borisevich, N. A.; Malkin, Y. N.; Ruziev, S.; Mel'nichuk, S. V.; Tikhomirov, S. A.; Tolstorozhev, G. B.; Kuz'min, V. A. *Izv. Akad. Nauk SSSR, Ser. Khim.* **1990**, *3*, 468−471.
(31) Scott, T. W.; Liu, S. N. *J. Phys. Chem.* **1989**, *93*, 1393−1396.
(32) Lembke, R. R.; Natarajan, L. V.; Kuntz, R. R. *J. Photochem.* **1983**, *21*, 814.
(33) Marqusee, S.; Robbins, V. H.; Baldwin, R. L. *Proc. Natl. Acad. Sci. U.S.A.* **1989**, *86*, 5286−5290.

conformation.[34] The carbonyl groups of the peptide backbone absorb at different frequencies in different hydrogen-bonding environments such as random coils, α-helix, and β-sheets.[35] Furthermore, transient optical spectroscopy can also be used for reasons stated above.

Here, we report the synthesis of potential cross-linking amino acids, (*S*)-4′-mercaptophenylalanine (thiotyrosine, Tty) and 3-*N*-(4′-mercaptophenyl)-*(S)*-2,3-diaminoproprionic acid (aminothiotyrosine, Aty), their incorporation into peptides, and the photochemical and biophysical characterization of the resulting peptides. Two peptides with the same sequence but two different thiol amino acids were examined. The kinetics of the early events of folding of these peptides will be reported elsewhere.[39]

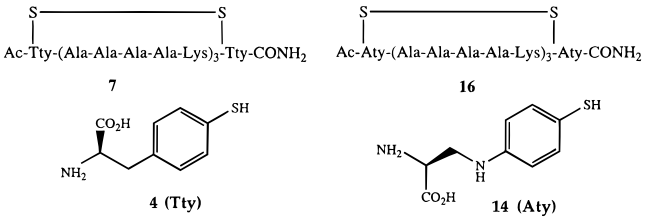

Results

Synthesis of Thiotyrosine 4 (Fmoc-Tty(4-MeBzl)) and Incorporation into Peptide 7. On the basis of the precedence of the photochemistry of diphenyl disulfide,[29−31] we envision that the thiotyrosine Tty might serve as the precursor to the aryl disulfide cross-linked peptide. Tty is structurally similar to thiophenol, and once oxidized should exhibit similar photochemistry and ultrafast photodissociation of the SS bond as observed for diphenyl disulfide. The synthesis[36] of Tty in properly protected forms for use in solid phase peptide synthesis is outlined in Scheme 2a. Starting from L-phenylalanine, chlorosulfonation gave rise to the unstable chlorosulfonyl derivative **1**. This compound was reduced to the air sensitive thiol **2** with powdered tin and hydrochloric acid. The thiol group of **2** was reacted with 4-methylbenzyl bromide to give the *S*-4-methylbenzyl (4-MeBzl) derivative **3**. The amino group of **3** was protected with 9-fluorenylmethyl group to afford amino acid **4** (Fmoc-Tty(4-MeBzl)), which is properly protected for use in solid phase synthesis using Fmoc[37] chemistry. The overall yield of Fmoc-Tty(4-MeBzl) is 30% from L-phenylalanine. The ease in which Fmoc-Tty(4-MeBzl) is prepared makes this compound an attractive precursor of the optical trigger.

Compound **4** was coupled to PAL resin using HBTU, and the remaining amino acids were coupled under standard conditions as described in the Experimental Section. We sought a thiol-protecting group that would be stable to the conditions required for cleavage from PAL resin to allow purification of the acyclic reduced form of the peptide **6**. Various thiol-protecting groups were investigated including *S*-benzyl, *S*-methoxybenzyl, *S*-acetamidomethyl, and *S*-methylbenzyl groups. The *S*-methylbenzyl group was found to yield the cleanest and highest yield of peptide **6** with the least amount of polymeric material arising from deprotection of the thiol group. Peptide **6** was oxidized to the cyclic disulfide cross-linked peptide **7** with DMSO as the oxidant[38] (Scheme 2b). Peptide **7** was purified by RP-HPLC and characterized by electrospray mass spectroscopy.

Scheme 2. Synthesis of (a) Fmoc-Tty (4-MeBz), **4**, and (b) Peptide **7**

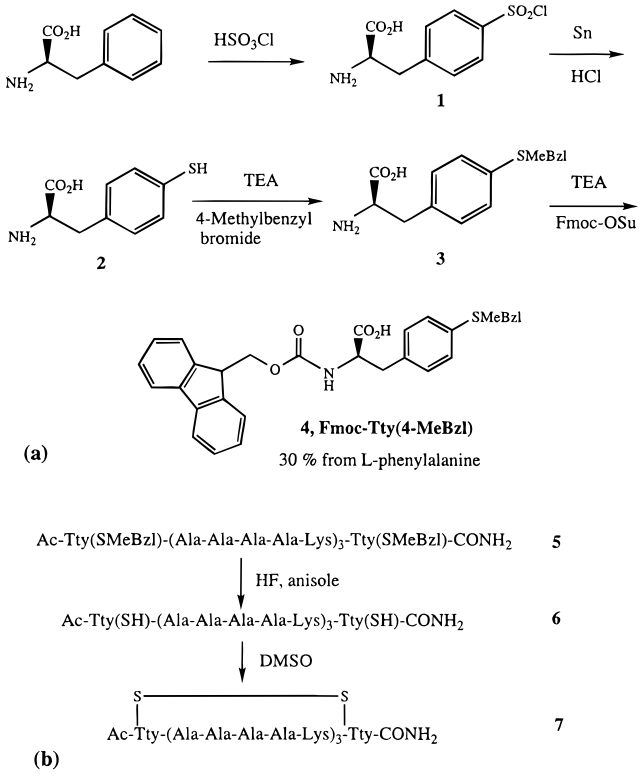

Photochemistry of Peptide 7. Peptide **7** was photolyzed at 270 nm, and the transient absorption spectrum was monitored. Immediately following photolysis, a transient was observed centered at 500 nm.[39] The absorption spectrum compares well with that from phenylthiyl radical, with a band centered around 450 nm.[31] This transient signal decays rapidly to 17% of the initial intensity at 50 ps and to 2% by 1 ns. We hypothesize that the absorbance decay of thiyl radicals derived from **7** is due to recombination based on kinetic studies of phenylthiyl radicals.[29−31] Following the photolysis of diphenyl disulfide, phenylthiyl radical is formed in less than 1 ps. The intensity of the thiyl absorption then diminishes to a plateau value of 15−75% in 1 ns depending on the solvent.[29] The fast, initial decrease in the absorbance of thiyl radical is attributed to cage (geminate) recombination, with a half-life for recombination in the tens of picosecond range. The remainder of the phenylthiyl radicals escape from the cage and give rise to the absorbance plateau. The thiyl radicals from peptide **7**, on the other hand, are tethered at the ends of the peptide chain. We propose that once the disulfide bond is cleaved, the peptide backbone of **7** has not had sufficient time to diffuse apart and holds the two thiyl radicals in close proximity and proper orientation for rapid recombination.

To overcome this unexpected obstacle, we sought various ways to increase the survival probability of the thiyl radicals generated from photolysis of the cross-linked polyalanine peptides. If the rate of recombination were sufficiently de-

(34) Locke, B.; Diller, R.; Hochstrasser, R. M. Wiley: New York, 1993; Vol. Part B, Vol. 20, pp 1−43.
(35) Krimm, S.; Bandekar, J. *Adv. Protein Chem.* **1986**, *38*, 181−364.
(36) Escher, E.; Bernier, M.; Parent, P. *Helv. Chim. Acta* **1983**, *66*, 1355−1365.
(37) Abbreviations: Fmoc, 9-fluorenylmethoxycarbonyl; PAL, 5-(4-(aminomethyl)-3,5-bis(methyloxy)phenoxy)valeric acid; TFA, trifluoroacetic acid; DMSO, dimethyl sulfoxide; HPLC, high-performance liquid chromatography; CD, circular dichroism; UV, ultraviolet; HBTU, *o*-benzotriazole-*N*,*N*,*N*′,*N*′-tetramethyluronium hexafluorophosphate; DIEA, *N*,*N*-diisopropylethylamine.
(38) Tam, J. P.; Wu, C. R.; Liu, W.; Zhang, J. W. *J. Am. Chem. Soc.* **1991**, *113*, 6657−6662.
(39) Volk, M.; Kholodenko, Y.; Lu, H. S. M.; Gooding, E.; DeGrado, W. F.; Hochstrasser, R. M. Submitted for publication in *J. Phys. Chem.*

Scheme 3. Synthesis of Aminothiotyrosine **14** and Peptide **16**

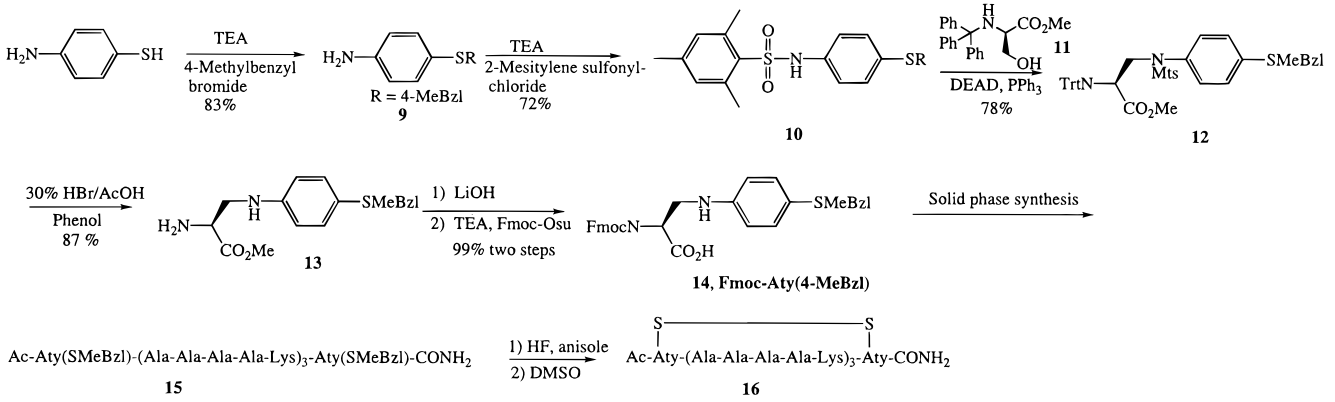

creased, the radicals might be able to diffuse apart, thereby allowing peptide folding to occur. The first approach we examined was to increase the steric bulk around the thiyl radical center. The steric hindrance was thought to prevent the two thiyl radical centers from approaching each other. Therefore, we determined the quantum yield of caged recombination of 2,3,5,6-tetramethylphenylthiyl and 2,4,6-triisopropylphenylthiyl and compared them with that of *p*-tolylthiyl. All three disulfides exhibited no observable difference in caged recombination quantum yield. Apparently, the additional steric hindrance did not appreciably slow down caged recombination.[40] Because the model disulfides looked unpromising, we did not investigate peptides with substituted thiotyrosine derivatives incorporated.

The second approach was to perturb the peptide conformation such that upon photocleavage of the SS bond the peptide changes its conformation more rapidly so that the two thiyl radicals are no longer in close proximity. Computer modeling using molecular dynamics simulation showed that the cyclic disulfide-containing peptide **7** samples multiple conformations. Many conformers show approximately two turns of helix with the aryl disulfide packed across the helix, possibly stabilizing it through favorable van der Waals and hydrophobic interactions. Such a low-energy conformation may be kinetically stable, leading to rapid recombination of the thiyl radicals once they are generated. Indeed, the mean residue ellipticity at 222 nm, $[\theta]_{222}$ of **7** was $-13\,700$ deg cm^2 dmol^{-1}, providing evidence for a partially helical conformation. We therefore prepared a second peptide **8**, which appeared to be less likely to adopt such a low-energy conformation as assessed by molecular dynamics simulation.

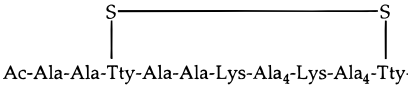

(8)

Although this peptide had a lower helical content as determined by CD spectroscopy ($[\theta]_{222} = -8300$ deg cm^2 dmol^{-1}), it exhibited a very rapid decay of thiyl absorbance similar to that of peptide **7**. Apparently, the structural perturbation of **8** was not sufficient to drive the necessary rapid change to a conformation nonproductive for thiyl radical recombination. For this approach to work, the conformational changes must be able to compete with the geminate recombination process, on the order of 50 ps. Our failure to effect a change in the recombination efficiency implies that no major reorganization of the peptide backbone occurs in 50 ps. This observation is consistent with the recent measurements of helix formation kinetics by Williams[24] and Thompson[41] on polyalanine peptides which showed that major backbone conformational changes have time constants of 30 and 160 ns.

The third approach we examined was to perturb the thiyl radical such that it might access an alternative excited state configuration which would not lead to caged recombination. It has been shown that *p*-amino-substituted diphenyl disulfides do not undergo geminate recombination following photolysis.[29,30] The rationale for this phenomenon is that the para amino group can form an intramolecular charge transfer complex with the thiyl radical center, decreasing the recombination probability of the geminate radical pairs, and reducing geminate recombination. With this precedent in mind, we set out to synthesize the *p*-amino analogue of Tty, compound Aty, where an amino group is inserted in the para position of the modified tyrosine.

Synthesis of Amino Acid 14 (Fmoc-Aty(4-MeBzl)) and the Incorporation into Peptide 16. Aminothiotyrosine Aty is a derivative of 2,3-diaminoproprionic acid, a class of compounds which we felt might be easily accessible in stereochemically pure form starting with a derivative L-serine. However, activation of the hydroxyl of L-serine is known to be problematic and leads to β-elimination product, dehydroalanine.[42,43] Arnolds reported the use of *N*-(*tert*-butoxycarbonyl)-L-serine lactone in preventing elimination and showed that various nucleophiles react at the β-carbon of L-serine lactone.[42] Unfortunately, *S*-(4′-methylbenzyl)-4-aminothiophenol failed to react with L-serine lactone in appreciable yield, presumably due to the poor nucleophilicity of the aniline group. We therefore turned to the Mitsunobu reaction using L-serine-*N*-trityl methyl ester (**11**). Bulky N-protecting groups are found to protect the α-center of amino acids from base-catalyzed racemization.[44,45] In particular, Cherney had reported that the trityl protecting group prevented β-elimination, thereby providing high yields of Mitsunobu addition products in a stereospecific manner.[46] Indeed, reaction of **11** with sulfonamide **10** under Mitsunobu conditions provided the desired addition product **12** in 78% yield. Acidolytic cleavage of the 2-mesitylenesulfonyl (Mts) and trityl protecting groups from **12** using 30% HBr in acetic acid, followed by saponification of the intermediate **13** and reaction of the product with (fluorenylmethyl)-*N*-hydroxysuccinimide, afforded the protected amino acid **14** (Fmoc-Aty(4-MeBzl)) (Scheme 3).

Amino acid **14** is properly protected for use in solid phase peptide synthesis, in an analogous manner as described previously for the preparation of peptide **7**. Although the β-amino

(40) The photochemistry of these disulfides will be reported elsewhere.
(41) Thompson, P. A.; Eaton, W. A.; Hofrichter, J. *Biophys. J.* **1996**, *70*, A177.
(42) Arnold, L. D.; Kalantar, T. H.; Vederas, J. C. *J. Am. Chem. Soc.* **1985**, *107*, 7105−7109.
(43) Mitsunobu, O. *Synthesis* **1981**, 1−28.
(44) Guthrie, R. D.; Nicolas, E. C. *J. Am. Chem. Soc.* **1981**, *103*, 4637−4638.
(45) Christie, B. D.; Rapoport, H. *J. Org. Chem.* **1985**, *50*, 1239−1245.
(46) Cherney, R. J.; Wang, L. *J. Org. Chem.* **1996**, *61*, 7544−7546.

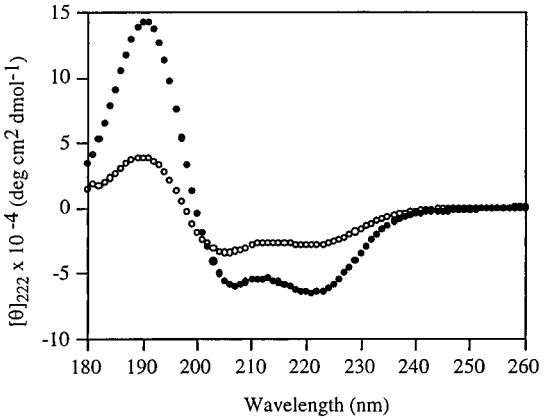

Figure 1. CD spectra of linear peptide **15** (●) and cyclic peptide **16** (○) at 1 °C. $[\theta]_{222}$ is −64 000 deg cm^2 dmol^{-1} for **15** and −28 000 deg cm^2 dmol^{-1} for **16**. The molar ellipticity at 222 nm for **15** is greater than that expected for a 100% helical peptide, presumbly due to the aromatic absorption of the amino thiotyrosine group.

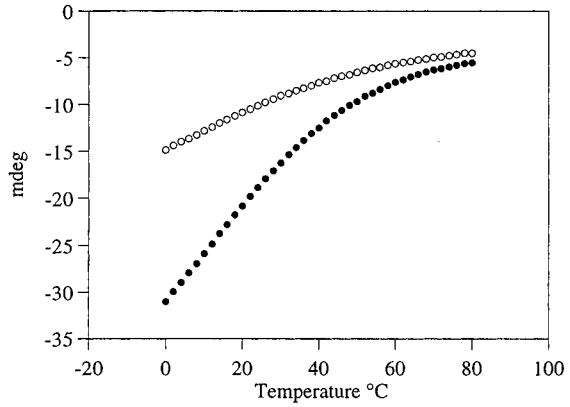

Figure 2. CD temperature melting curves of linear peptide **15** (●) and cyclic peptide **16** (○).

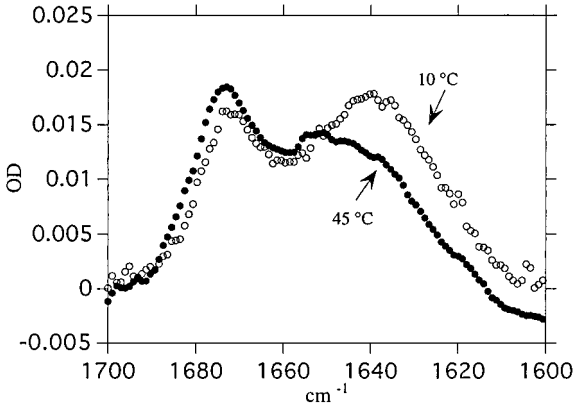

Figure 3. FT-IR spectra of linear peptide **15** at 10 °C (○) and 44 °C (●) in D_2O. Each spectrum was obtained by subtracting the D_2O spectrum from the peptide spectrum at that temperature.

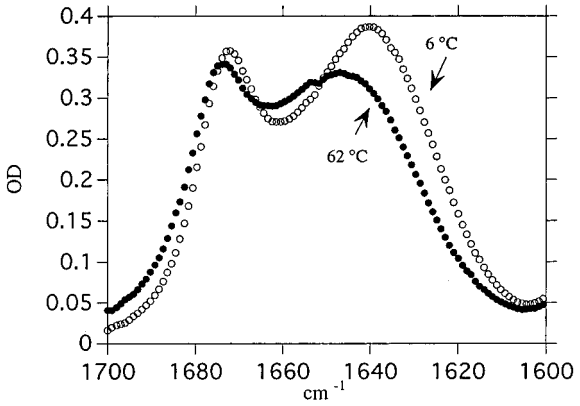

Figure 4. The IR spectra of **16** at 6 °C (○) and 62 °C (●) in D_2O. Each spectrum was obtained by subtracting the D_2O spectrum from the peptide spectrum at that temperature.

group was not protected, the solid phase peptide synthesis proceeded smoothly to yield the *S*-methylbenzyl-protected peptide **15**. Evidently, the low reactivity of the aniline obviates the need for protection. Peptide **15** was treated with HF and oxidized with DMSO to yield the desired cyclic peptide **16**. Peptide **16** was purified by RP HPLC on preparative C18 Vydac column and characterized by electrospray mass spectroscopy.

Secondary Structure of Cyclic Peptide 16 and Linear Peptide 15. From CD spectroscopy, we can analyze the changes in the secondary structure expected to occur upon photocleavage of cyclic peptide **16**. Linear peptide **15** was used to model the folded conformation after photocleavage of **16**. The CD spectra of the two peptides at the same concentrations are shown in Figure 1. From the minimum at 222 nm band and the maximum at 190 nm band, it is clear that disulfide cross-linked peptide **16** has helical regions. It is difficult to determine the fractional helicity of **16** since the aminothiophenol moiety of the modified tyrosine unit most likely contributes to the absorption in this region, as previously observed for other peptides containing aromatic residues.[47] The linear peptide **15** exhibits considerably greater helical character based on the intensity of the 222 nm band. Assuming that the helical content is linearly related to the intensity of the 222 nm band, linear peptide **15** has approximately twice the helicity of the cyclic peptide. Therefore, upon photocleavage of cyclic peptide **16**, it is reasonable to expect it to fold into a more helical peptide conformation.

The temperature dependence of the secondary structure of **15** and **16** was examined by CD (Figure 2). Both peptides showed a broad melting curve, commonly observed for short peptides. The secondary structure of the cyclic peptide **16** is much less temperature dependent than that of the linear peptide **15**. This difference in temperature dependence of the two peptides can be exploited for future experiments. It would be desirable to conduct experiments at low temperatures to maximize the difference in the conformations of the cyclic and ring-opened peptides.

We also examined the infrared spectra of linear peptide **15** (Figure 3) and the cyclic peptide **16** (Figure 4) in D_2O as a function of temperature. For both peptides, two major peaks are observed in the amide I′ region (the prime indicates a deuterated amide). The peak at 1672 cm^{-1} is attributable to the CO absorption of the trifloroacetate counterion, and the 1640 cm^{-1} peak corresponds to the CO absorption of peptides in a helical conformation. These spectra agree well with that reported for a 21 residue polyalanine peptide.[24] At 10 °C, peptide **15** has a predominant peak centered at 1640 cm^{-1}, indicating that the linear peptide is in a mostly helical conformation at this temperature. Upon heating to 62 °C, a new peak at 1655 cm^{-1} is observed, in place of the 1640 cm^{-1} band. We attribute this temperature dependence to helix melting. With increasing temperature, the helix melts and gives rise to an ensemble with greater random coil content, resulting in the new peak at 1655 cm^{-1}. The same trend is observed upon heating of the crosslinked peptide **16** (Figure 4), indicating there is some residual helicity in the cyclic peptide as seen in the CD experiment, and the helical conformer melts upon

(47) Chakrabartty, A.; Kortemme, T.; Padmanabhan, S.; Baldwin, R. L. *Biochemistry* **1993**, *32*, 5560−5565.

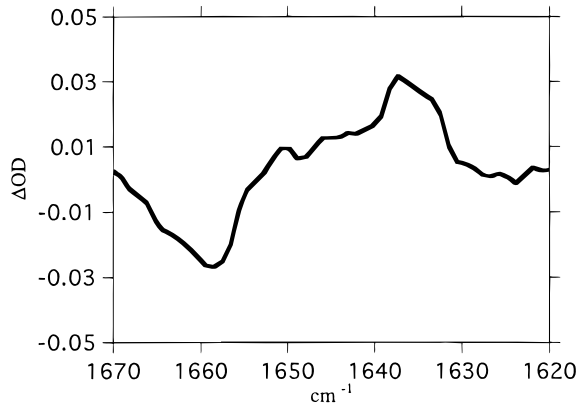

Figure 5. Difference spectrum of cyclic peptide **16** subtracted from that of linear peptide **15** in the amide I′ region at 10 °C. Because of the different concentrations of the two peptides used in the measurements, the spectra of **15** and **16** were normalized using TFA as the internal standard (TFA is present in the same molar ratio in both peptide samples).

heating. These changes in the IR spectra are very similar to changes observed for a 21-residue polyalanine peptide.[24]

To model the expected IR spectral changes upon photocleavage of peptide **16**, the IR spectrum of **16** was compared with that of the linear peptide **15**. The difference spectra of cyclic peptide **16** subtracted from that of linear peptide **15** at 10 °C is shown in Figure 5. In the amide I′ region, conformational changes resulting from the cleavage of the SS bond lead to an increase in intensity of the CO absorption in the helical region concomitant with a decrease in intensity of the CO absorption in the coil region. These IR data are consistent with the CD data and indicate that the designed structural change of the peptide upon SS bond cleavage has been fulfilled.

Photochemistry of Cyclic Peptide 16. Peptide **16** was photolyzed at 270 nm, and the transient absorption recorded. Analogous to thiotyrosine-containing peptide **7**, transient absorption at 580 nm was observed immediately upon photolysis of peptide **16**. A rapid decay is observed in the first 50 ps, during which 53% of the initial thiyl absorbance is consumed, presumably due to geminate recombination. However, in contrast to peptide **7**, the residual transient signal then decays in a relatively slow, nonexponential manner from tens of picoseconds to microseconds. For example, at 2 and 50 ns respectively, 20 and 9% of the transient absorption can still be detected. Thus, the introduction of an amino substitution para to the thiol group leads to a significant percentage of long-lived thiyl radicals, allowing peptide folding to take place. The thiyl radicals at the ends of the peptide chain can diffuse apart to give long-lived transients in the nanosecond time scale. This increase in radical lifetime should allow for the observation of protein dynamics in the time range of picoseconds to hundreds of nanoseconds.

Discussion

We have investigated the feasibility of using an aryl disulfide cross-linking group as a sub-picosecond optical trigger for protein folding. Our initial study using thiol-tyrosine as the optical trigger yielded the unexpected result that the peptide chain constrains the two incipient thiyl radicals in spatial proximity for efficient recombination. On the basis of previous studies of thiyl radical recombination and our own observations, we can estimate that no peptide motions significant to radical diffusions occurred before 50 ps. These results are also consistent with the absorption anisotropy decay of thiyl radicals derived from cyclic peptide **16**, which indicated that overall peptide rotation occurs with a lifetime of 600 ps.[39]

Scheme 4

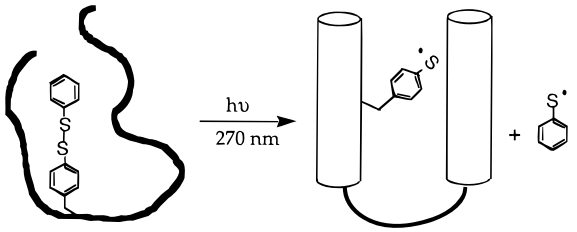

To increase the lifetime of the thiyl radicals, we designed the amino acid Aty, which contains a radical-stabilizing amino group para to the thiol. This is the first optically triggered cross-linking agent which allows for the detection of protein dynamics from picoseconds to microseconds. It also meets nearly all of our design criteria: (1) it is easily prepared in protected form in six steps in 40% overall yield; (2) it can be incorporated into peptides and proteins by routine solid phase methods; (3) it is cleaved in less than a picosecond, allowing the full range of protein dynamics to be examined, from extremely fast to slow conformational processes; (4) it has a high cleavage quantum yield; (5) photocleavage is readily and rapidly reversible, enabling data averaging for good signal-to-noise ratios; (6) photocleavage creates a very strongly absorbing chromophore that acts both as a probe of protein dynamics as well as a monitor of the photocleavage and recombination processes. The sole feature that has not yet been optimized is the degree of recombination occurring on a time scale faster than backbone conformational changes (in this case, approximately 10−100 ns[24,41]). In the current study, approximately 70−80% of the radicals rapidly recombine within 2 ns. Nevertheless, this yield has proven adequate to allow in-depth study of conformational processes in peptide **16**.[39]

One major area of future research would be to further stabilize the lifetime of the radicals. For example, it may be possible to attach a triplet sensitizer onto or adjacent to Aty. One could then photolyze the triplet sensitizer chromophore selectively, which would then transfer energy intramolecularly to the thiyl chromophore, and lead to cleavage of the disulfide bond in the triplet state.[48] Then, the two triplet thiyl radicals would be prevented from rapid recombination by the spin barrier, thereby increasing their lifetime. The photophysics of such a system is more complicated and less direct than that of Aty, but may be well worthy of an investigation to increase the efficiency of our triggering methodology.

Aty may find broad applications for a variety of studies of peptide and protein conformational change. In the current work, we demonstrate that a cyclic Aty disulfide can constrain a peptide to a nonhelical conformation, which relaxes to a helix upon cleavage to the linear form. In a similar manner, one might use this group to initiate folding of an entire protein through the incorporation of an intramolecular disulfide bond that destabilizes the native fold. Alternatively, another application could involve incorporating Aty in the protein interior and forming a mixed disulfide with an extraneous sulfhydryl group. The presence of the extraneous group might prevent the protein from folding. Upon photocleavage of the disulfide bond, the extraneous thiyl group would then diffuse away, and the protein would begin to fold (Scheme 4).

Experimental Section

Materials and Methods. Reagents and solvents were obtained from commercial sources and used without purification. Fmoc-protected

(48) Turro, N. J. *Modern Molecular Photochemistry*; University Science Books: Mill Valley, 1991.

amino acids and PAL resin were purchased from PerSeptive Biosystems. NMR spectra were obtained on a Bruker AMX 300, with TMS or acetone as the internal standard. Mass spectra were obtained using a VG Zab-E double-focusing mass spectrometer using a Xenon FAB gun as the ion source or on a Finnigan MAT 8230. CD spectra were obtained using an AVIV 62A DS system. FT-IR spectra were collected with a Bruker IFS 66 system. Analytical HPLC was performed on Vydac C_{18} reverse phase column (25 × 0.46 cm i.d.) with a flow rate of 0.5−1.0 mL/min, monitored at 220 nm. Peptides were purified using Rainin or Waters HPLC equipment on a Vydac C_{18} reverse phase column (25 × 2.5 cm i.d.) with a flow rate of 10 mL/min, monitored at 220 nm. Eluent used were (A) 0.1% TFA in water and (B) 0.1% TFA in 90% acetonitrile, 9.9% H_2O.

Peptide Synthesis. Peptides were all synthesized using standard Fmoc chemistry and the stepwise solid phase method on PAL resin using a Milligen Model 9050 peptide synthesizer. Couplings of the commonly occurring Fmoc-L-amino acid pentafluorophenyl esters were accomplished using 1-hydroxybenzotriazole hydrate in DMF, and Fmoc-L-amino acids were coupled using HBTU/DIEA in DMF as a catalyst. In general, 4 equiv of commercially available amino acids (based on loading of the resin) were used. The amino acids were circulated through the resin for 45 min, and the unnatural amino acid was double coupled. To stabilize helix formation, end charges were neutralized by acetylating the N-terminus and amidating the C-terminus of the peptide. Peptides were cleaved from the resin by stirring the dried resin for 2 h at room temperature with 9:0.5:0.3:0.2 TFA:thioanisole:ethanedithiol:anisole mixture. The mixture was filtered and concentrated under a nitrogen stream. The filtrate was triturated with cold ether, and crude peptide was filtered and collected. The crude peptide was purified to greater than 95% purity using a 2.5 cm Vydac C_{18} RP column.

Ac-Tty(S-4-MeBzl)-(Ala-Ala-Ala-Ala-Lys)$_3$-Tty(S-4-MeBzl)-CONH$_2$ (5). Thiotyrosine **4** (2 equiv per resin) was attached to PAL resin (Perceptive Biosystem, 0.6 g, 0.38 mmol/g) by coupling with HBTU/DIEA (1.2 equiv) for 45 min and then repeating this reaction to couple unreacted amino group. Subsequent amino acids were added as described above. The crude peptide was isolated as described above and purified to greater than 95% pure. HPLC retention time: 48.3 (0−60% B/60 min). Mass spectrum (ESI): *m/z* 1862.0 [(M + H)$^+$, calcd 1862.6].

Ac-Tty(SH)-(Ala-Ala-Ala-Ala-Lys)$_3$-Tty(SH)-NH$_2$ (6). Peptide **5**, purified or crude, was treated with anhydrous hydrogen fluoride containing anisole (1 mL per gram of peptide cleaved) as scavenger at 0 °C for 1 h to remove the *p*-methylbenzyl protecting group. The crude product was triturated with ether and purified by RP HPLC on a 2.5 cm Vydac C18 column, using gradient condition 25−55% B/60 min, flow rate = 10 mL/min. The purified yield of **6** was 10% from starting material. HPLC retention time: 37.0 min (0−60% B/60 min). Mass spectrum (ESI): *m/z* 1654.1 [(M + H)$^+$, calcd 1653.8].

Cyclo-[Ac-Tty(S)-(Ala-Ala-Ala-Ala-Lys)$_3$-Tty(S)-CONH$_2$] Disulfide (7). Peptide **6** (10 mg) was dissolved in 5% acetic acid (10 mL). The pH of the solution was adjusted to 4 by addition of ammonium hydroxide. DMSO (2 mL) was added, and the mixture was stirred at room temperature for 8 h. HPLC analysis showed that the oxidation is complete at this time. The solution was frozen and lyophilized. The crude peptide was purified by RP HPLC on a Vydac C18 column with eluting gradient of 20−40% B/50 min. Purified yield: 7.0 mg (70%). HPLC retention time: 32.4 min (0−60% B/60 min). Mass spectrum (ESI): *m/z* 1651.8 [(M + H)$^+$, calcd 1652.8].

Ac-Aty(S-4-MeBzl)-(Ala-Ala-Ala-Ala-Lys)$_3$-Aty(S-4-MeBzl)-CONH$_2$ (15). This peptide was prepared as described for peptide **5**. HPLC retention time: 24.2 min (10−100%B/45 min). Mass spectrum (ESI): *m/z* 1892.6 [(M + H)$^+$, calcd 1892.0].

Ac-Aty(SH)-(Ala-Ala-Ala-Ala-Lys)$_3$-Aty(SH)-CONH$_2$. This peptide was prepared as described for peptide **6**. HPLC retention time: 17.1 (10−100% B/45 min). Mass spectrum (ESI): *m/z* 1684.0 [(M + H)$^+$, calcd 1683.9].

Cyclo-[Ac-Aty(S)-(Ala-Ala-Ala-Ala-Lys)$_3$-Aty(S)-CONH$_2$] Disulfide (16). This peptide was prepared as described for peptide **7**. HPLC retention time: 15.7 min (10−100% B/45 min). Overall yield of **16** from 0.2 mmol of PAL resin was 10%. Mass spectrum (ESI): *m/z* 1682.6 [(M + H)$^+$, calcd 1681.9].

(*S*)-*S*-(4-Methylbenzyl)-*N*-(fluorenylmethyloxycarbonyl)-4′-mercaptophenylalanine (Fmoc-Tty(4-MeBzl), 4). This compound was prepared in a four-step procedure beginning with L-phenylalanine. Due to the air sensitive nature and limited solubility of the intermediates, the reactions were run in succession and only the final product was fully characterized.

(*S*)-4′-Mercaptophenylalanine (2). Using a modified procedure of Escher et al.,[36] L-phenylalanine (5.0 g, 30 mmol) was added to a dried 250 mL three-neck round bottom flask, cooled to −15 °C, and stirred with a mechanical stirrer. To this was added dropwise via an additional funnel chlorosulfonic acid (30 mL, 450 mmol), precooled to −15 °C, under nitrogen. After addition, the mixture was warmed to room temperature and stirred for 4 h under nitrogen. The resulting light brown mixture was then added slowly via an additional funnel to a two-neck flask containing 75 g of ice and 20 mL of H_2O with vigorous stirring, and the mixture was cooled with an ice bath, such that the temperature of the mixture is maintained at less than 10 °C. A white solid, the salt of the 4′-chlorosulfonyl derivative of L-phenylalanine, precipitated during the addition. While the reaction vessel was kept at less than 10 °C, concentrated HCl (30 mL) was added, followed by Sn powder (17.8 g, 150 mmol). The mixture was brought to reflux for 2 h and then cooled to room temperature. The solution was diluted with 300 mL of H_2O, and H_2S was bubbled through the mixture until no more tin sulfide is precipitated. The solution was filtered, and the filtrate was concentrated to approximately 100 mL under reduced pressure. The resulting air sensitive thiol **2** was used immediately without further characterization.

(*S*)-*S*-(4-Methylbenzyl)-*N*-(fluorenylmethyloxycarbonyl)-4′-mercaptophenylalanine (3). The solution of crude thiol **2** was neutralized with 4 N NaOH on an ice bath and diluted with 250 mL of EtOH. To this suspension were added triethylamine (10.4 mL, 76 mmol) and α-bromo-*p*-xylene (3.16 g, 17 mmol). The mixture was stirred at room temperature overnight. The crude mixture was filtered, concentrated to 200 mL, and cooled to 0 °C. An off-white solid precipitated and was collected by filtration to yield 4.1 g of crude product. The filtrate was further concentrated to 100 mL and cooled to 0 °C. Another 0.9 g of off-white solid precipitated out and was collected and combined with the first batch of products to give a total of 5.0 g (97%) of crude product.

(*S*)-*S*-(4-Methylbenzyl)-*N*-(fluorenylmethyloxycarbonyl)-4′-mercaptophenylalanine (4). Crude **3** (5.0 g, 17 mmol) was suspended in 17 mL of water and 25 mL of acetonitrile. Triethylamine (1.7g, 17 mmol) was added, followed by 9-(fluorenylmethyloxycarbonyl)-*N*-hydroxysuccinimide (5.6g, 17 mmol), and the mixture was stirred overnight. The pH of the reaction mixture was maintained at 8.5−9.0 by addition of triethylamine. The crude mixture was poured into 20 mL of 1.5 N HCl and 20 mL of ethyl acetate, and layers separated. The aqueous layer was extracted with ethyl acetate (3 × 100 mL), and the organic layers were combined, washed with brine, dried over $MgSO_4$, and concentrated *in vacuo* to give a yellow oil. The crude product was purified by flash column chromatography on silica gel, using 100:5:1 methylene chloride:methanol:acetic acid as the eluent. After purification, 4.6 g (53%) of white solid was obtained. ^{1}H NMR (300 MHz, acetone-d_6): δ 7.85 (d, J = 7.5 Hz, 2H), 7.65 (m, 2H), 7.42−7.13 (m, 10 H), 7.08 (d, J = 7.5 Hz, 2H), 6.73 (d, J = 8.6 Hz, 1H), 4.50 (m, 1H), 4.31−4.12 (m, 4H), 4.08 (s, 2H), 3.8 (broad, 1H), 3.23 (m, 1H), 3.00 (m, 1H), 2.25 (s, 3H). ^{13}C NMR (500 MHz, acetone-d_6): δ 173.06, 156.80, 144.96, 142.02, 137.31, 136.35, 135.85, 130.73, 129.79, 129.57, 128.50, 127.89, 126.13, 120.74, 67.14, 55.89, 47.96, 38.56, 37.68, 21.03. HRMS: calcd for $C_{32}H_{29}NO_4S$ (M + Na)$^+$ 546.1716, found 546.1730.

4-Amino-*S*-(4-methylbenzyl)mercaptobenzene (9). Triethylamine (37.0 g, 370 mmol) was added to a stirred solution of 4-aminothiophenol (50 g, 90% purity, 370 mmol) dissolved in 360 mL of EtOH. To this was added α-bromo-*p*-xylene (68.5 g, 370 mmol). The mixture was stirred at room temperature for 18 h. The solvent was removed *in vacuo* to yield a yellow oil. The oil was dissolved in CH_2Cl_2 (300 mL), washed with H_2O (500 mL) and saturated sodium bicarbonate solution (500 mL), dried over $MgSO_4$, and concentrated. The crude product was purified by flash column chromatography on silica gel using 1:5 ethyl acetate:hexane as the eluent to give a pale yellow solid (41.1 g, 83%). ^{1}H NMR (300 MHz, $CDCl_3$): δ 7.20 (2H, d, J = 9

Hz) , 7.13 (4H, dd, $J = 6$, 15Hz), 6.65 (2H, d, $J = 9$ Hz), 4.65 (br s, 2H), 3.97 (s, 2H), 2.30 (s, 3H). ^{13}C NMR (500 MHz, $CO(CD_3)_2$): 148.9, 136.8, 135.1, 132.5, 130.2, 121.8, 114,1, 41.8, 21.1. HRMS: calcd for $C_{14}H_{15}NS$ $(M + H)^+$ 229.0925, found 229.0921.

4-[(2-Mesitylenesulfonyl)amino]-1-[(*p*-methylbenzyl)thio]benzene (10). Triethylamine (7.8 g, 78 mmol) was added to a stirred solution of **9** (7.0 g, 31 mmol) in 30 mL of CH_2Cl_2. To this was added 2-mesitylenesulfonyl chloride (8.5 g, 39 mmol), and the solution was stirred at room temperature for 18 h. The solvent was evaporated *in vacuo*. The crude product was dissolved in ethyl acetate (500 mL), washed with 10% HCl solution (5 × 500 mL), dried over $MgSO_4$, and concentrated. Purification of the crude product was achieved by flash column chromatography on silica gel using 1:5 ethyl acetate:hexane as the eluent and yielded 9.0 g (72%) of white solid. ^{1}H NMR (300 MHz, $CDCl_3$): δ 7.18 (d, 2H, $J = 9$ Hz), 7.08 (m, 4H), 6.91 (s, 2H), 6.84 (d, 2H, $J = 9$ Hz), 6.43 (br s, 1H), 3.98 (s, 2H), 2.57 (s, 6H), 2.31 (s, 3H), 2.28 (s, 3H). ^{13}C NMR (500 MHz, $CO(CD_3)_2$): δ 143.1, 141.9, 139.9, 137.2, 137.0, 135.4, 135.0, 132.6, 131.6, 129.7, 129.5, 121.7, 39.0, 23.0, 21.0, 20.8. HRMS: calcd for $C_{23}H_{25}NO_2S_2$ $(M + NH_4)^+$ 429.1671, found 429.1665.

2-*N*-Trityl-3-*N*-(2-mesitylenesulfonyl)-3-*N*-[4′-[(4-benzylmethyl)thio]phenyl]-*(S)*-2,3-diaminopropionate Methyl Ester (12). *N*-Trityl-L-serine methyl ester (**11**) (5.5 g, 15 mmol) was dissolved in 100 mL of anhydrous benzene and stirred at room temperature under nitrogen. To this was added **12** (5.2g, 13 mmol) followed by triphenylphosphine (4.4 g, 17 mmol). The mixture was stirred at room temperature for 5 min. Diethyl azodicarboxylate (2.6 mL, 17 mmol) was added dropwise via syringe under nitrogen. The reaction mixture was stirred for 24 h at room temperature. Solvent was removed *in vacuo* to yield a yellow oil. The crude product was purified by flash column chromatography on silica gel using 1:7 ethyl acetate:hexane as the eluent initially and then stepping the eluent to 1:5 ethyl acetate: hexane. A white solid (7.4 g, 78%) was obtained after purification. ^{1}H NMR (300 MHz, $CO(CD_3)_2$): δ 7.39 (m, 6H), 7.21 (m, 17H), 6.93 (s, 2H), 4.20 (m, 2H), 4.12 (s, 2H), 3.41 (m, 1H), 3.13 (s, 3H), 2.43 (s, 6H), 2.31 (s, 3H), 2.23 (s, 3H). ^{13} C NMR (500 MHz, $CO(CD_3)_2$): δ 173.74, 146.74, 143.63, 141.14, 138.20, 137.66, 137.58, 135.26, 133.82, 132.78, 132.21, 130.39, 130.06, 129.66, 129.55, 128.78, 128.21, 127.39, 125.81, 72.18, 55.82, 56.74, 55.31, 52.14, 38.39, 30.44, 30.28, 23.62, 21.45, 21.19. HRMS: calcd for $C_{46}H_{46}N_2O_4S_2$ $(M + Na)^+$ 777.2197, found 777.2181.

3-*N*-[4′-[(4-Benzylmethyl)thio]phenyl]-*(S)*-2,3-Diaminopropionate Methyl Ester (13). To a 100 mL round bottom flask containing compound **12** (3.6 g, 4.8 mmol) was added phenol (13 g), followed by 50 mL of 30% HBr in acetic acid. The mixture was stirred at room temperature for 15 h. Excess HBr was blown into a H_2O trap under a stream of nitrogen. The reaction mixture was concentrated *in vacuo* to 5−7 mL. Ether, precooled to −78 °C, was added to yield an orange precipitate. The precipitate was collected by filtration and washed with cold ether (2 × 50 mL). The solid was dissolved in 200 mL of ethyl acetate and 200 mL of saturated sodium bicarbonate. The layers were separated, and the aqueous layer was extracted with ethyl acetate (2 × 100 mL). The organic layers were combined, dried over $MgSO_4$, and concentrated. The crude product was purified by flash column chromatography on silica gel, using 100:5 methylene chloride:methanol as the eluent, to yield 1.2 g (87%) of yellow oil. ^{1}H NMR (300 MHz, $CO(CD_3)_2$): δ 7.13 (d, 2H, $J = 9$ Hz), 7.08 (m, 4H), 6.61 (d, 2H, $J = 9$ Hz), 5.14 (br m, 1H), 3.92 (s, 2H), 3.41 (m, 1H), 3.20 (m, 1H), 2.84 (br s, 1H), 2.28 (s, 3H), 1.78 (br, 2H). ^{13}C NMR (500 MHz, $CO(CD_3)_2$): δ 171.9, 149.0, 136.7, 135.2, 134.2, 129.6, 121.8, 114.0, 63.0, 52.0, 46.8, 41.7, 21.0. HRMS: calcd for $C_{18}H_{22}N_2O_2S$ $(M + H)^+$ 331.1480, found 331.1492.

2-*N*-(Fluorenylmethyloxycarbonyl)-3-*N*-[4′-[(4-benzylmethyl)thio]-phenyl]-*(S)*-2,3-diaminoproprionic Acid (Fmoc-Aty(4-MeBzl), 14). Compound **13** (1.2 g, 3.8 mmol) was dissolved in 35 mL of acetonitrile and 20 mL of H_2O. To this was added lithium hydroxide (0.25 g, 5.9 mmol). The solution was stirred at room temperature for 15 h. The solution was neutralized with 10% HCl solution. To this was added 9-(fluorenylmethyloxycarbonyl)-*N*-hydroxysuccinimide, followed by triethylamine (0.42 g, 4.1 mmol), and the mixture was stirred at room temperature for 3.5 h. The pH of the mixture was maintained at 8−9. The solution was diluted with 200 mL of ethyl acetate and 200 mL of H_2O and acidified with 10% HCl solution. The layers were separated, and the aqueous layer was extracted with ethyl acetate (2 × 200 mL). The ethyl acetate layers were combined, dried over $MgSO_4$, and concentrated. The crude product was purified by flash column chromatography using 100:7.5:1 methylene chloride:methanol:acetic acid as the eluent to yield 2.0 g (two steps from **7**, 99%) of white solid. ^{1} H NMR (300 MHz, $CO(CD_3)_2$): δ 7.82 (2H, d, $J = 8$ Hz), 7.08 (2H, d, $J = 7$ Hz), 7.35 (m, 4H), 7.05 (d, 2H, $J = 9$ Hz), 7.07 (dd, 2H, $J = 7$, 8 Hz), 6.80 (br, 1H), 6.66 (2H, d, $J = 9$ Hz), 4.53 (m, 1H), 4.34 (d, 2H, $J = 7$ Hz), 4.24 (m, 1H), 3.92 (s, 2H), 3.60 (m, 2H), 2.26 (s, 3H). ^{13}C NMR (500 MHz, $CO(CD_3)_2$): δ 172.63, 157.12, 148.86, 145.08, 142.14, 137.00, 136.64, 135.11 (2 C's), 129.70, 128.60, 128.03, 126.18, 122.47, 120.84, 114.08, 67.36, 54.50, 48.06, 45.72, 41.76, 21.13.

Circular Dichroism. Spectra were recorded on an Aviv 62 DS spectropolarimeter. A circulating water bath was used to control the temperature. Concentrations of the stock peptide solutions were determined in duplicates or triplicates by amino acid analysis.

FT IR. Spectra were recorded on a Bruker IFS 66 equipped with a liquid N_2 MCT detector. A temperature-controlled cell with CaF_2 windows and adjustable pathlength, set at 50 μm, was used. At each temperature, the sample spectrum was corrected for D_2O absorption. For the measurements of peptide **16**, a stock solution of 13 mg/mL in D_2O was made just prior to the experiment. Due to the hydrophobic protecting group, 4-methylbenzyl, the same concentration of peptide **15** could not be achieved. Instead, a saturated solution of **15** in D_2O was used. The difference spectra of **15** and **16** were scaled using TFA as the internal standard.

Modeling. Modeling was carried out using Insight II (Biosym/MSI, San Diego, CA) on a Silicon Graphics Personal Iris. Energy minimization and molecular dynamics simulations were carried out using Discovery 3.0. The initial peptide structures were generated in InsightII using Biopolymer. Minimization and molecular dynamics calculations were carried out using constant dielectric of 1. The structures were minimized first using 1000 cycles of steepest descent and 10 000 cycles of conjugate gradients. Starting from these structures, molecular dynamics simulation were carried out by first equilibrating at 120 K for 500 fs (1 fs step size) and running dynamics for 20 ps, collecting structures every 2.5 ps. The resulting structures from dynamics were then subjected to minimization (1000 steps of steepest descent and 20 000 steps of conjugate gradients). This process was also repeated at 300 K. The structures were pooled and superimposed. Dynamic runs at 120 and 300 K gave the same gross structural features such as helical content of the peptides.

Acknowledgment. H.S.M.L. was supported in part by the Dupont Merck Postdoctoral Program. We thank Mary Boyd and Robert Cherney for helpful discussions and Joel Schneider and Blake Hill for critical reading of the manuscript. We thank Steve Koch for providing 2,3,5,6-tetramethylphenyl disulfide and 2,4,6-triisopropylphenyl disulfide.

JA970567O